Title

Expression of an Activated Integrin Promotes Long-distance Sensory Axon Regeneration in the Spinal Cord

Authors

Menghon Cheah[1], Melissa R. Andrews[2,*], Daniel J. Chew[1], Elizabeth B. Moloney[3], Joost Verhaagen[3], Reinhard Fässler[4], James W. Fawcett[1,*]

Affiliations

[1]John van Geest Centre for Brain Repair, University of Cambridge, Cambridge CB2 0PY, United Kingdom.

[2]School of Medicine, University of St. Andrews, St. Andrews KY16 9TF, United Kingdom.

[3]Laboratory for Neuroregeneration, Netherlands Institute for Neuroscience, 1105 BA, Amsterdam, Netherlands.

[4]Department of Molecular Medicine, Max Planck Institute of Biochemistry, 82152 Martinsried, Germany.

*Co-correspondence: M.R.A. (mra5@st-andrews.ac.uk), J.W.F. (jf108@cam.ac.uk)

Acknowledgements

This work was supported by grants from the Christopher and Dana Reeve Foundation, the Medical Research Council, the European Research Council ECMneuro, the Cambridge NHMRC Biomedical Research Centre.

Conflict of Interests

James Fawcett is a paid consultant for Acorda Therapeutics and Novartis.

Running title

Integrin Activation Promotes Axon Regeneration

Number of pages – 34 (excluding figures and legends)

Number of figures - 11

Number of words

Abstract - 164

Introduction – 648

Discussion - 1451

Abstract

After central nervous system injury, axon regeneration is blocked by an inhibitory environment consisting of the highly-upregulated tenascin-C and chondroitin sulfate proteoglycans (CSPGs). Tenascin-C promotes growth of axons if they express a tenascin-binding integrin, particularly α9β1. Additionally, integrins can be inactivated by CSPGs and this inhibition can be overcome by the presence of a β1-binding integrin activator, kindlin-1. We examined the synergistic effect of α9 integrin and kindlin-1 on sensory axon regeneration in adult rat spinal cord after dorsal root crush and adeno-associated virus transgene expression in dorsal root ganglia. After twelve weeks, axons from C6-C7 dorsal root ganglia regenerated through the tenascin-C-rich dorsal root entry zone (DREZ) into the dorsal column up to C1 level and above (over 25 mm axon length) through a normal pathway. Animals also showed anatomical and electrophysiological evidence of reconnection to the dorsal horn, and behavioral recovery in mechanical pressure, thermal pain and ladder-walking tasks. Expression of α9 integrin or kindlin-1 alone promoted much less regeneration and recovery.

Significance statement

The study demonstrates that long-distance sensory axon regeneration over a normal pathway and with sensory and sensory-motor recovery can be achieved. This was achieved by expressing an integrin that recognizes tenascin-C, one of the components of glial scar tissue, and an integrin activator. This enabled extensive long-distance (over 25 mm) regeneration of both myelinated and unmyelinated sensory axons with topographically correct connections in the spinal cord. The extent of growth and recovery we have seen would probably be clinically significant. Restoration of sensation to hands, perineum and genitalia would be a significant improvement for a spinal cord injured patient.

Introduction

After injury, central nervous system (CNS) axons fail to regenerate due to the presence of inhibitory factors, the lack of growth-promoting factors in the environment, and a poor intrinsic regenerative response of the neurons. In the injured CNS, extracellular matrix molecules such as chondroitin sulfate proteoglycans (CSPGs) and tenascin-C are highly upregulated and these molecules play a critical role in blocking CNS repair. The upregulated CSPGs in the glial scar have an inhibitory effect on axon growth and treatments directly targeting CSPGs, such as chondroitinase, can permit some axon regeneration (Friedlander et al., 1994, Bradbury et al., 2002, Moon et al., 2001, Cafferty et al., 2007). Tenascin-C has several splice variants containing the binding sites for CSPGs, integrins, fibronectin, laminin, contactin and other ligands (Joester and Faissner, 1999, Lundell et al., 2004, Probstmeier and Pesheva, 1999). The combination of CSPGs, tenascin-C, Nogo-A, semaphorin 3A and other inhibitory molecules forms an inhibitory environment for axon regeneration (Milev et al., 1997, Probstmeier et al., 2000, Kwok et al., 2014, Pasterkamp and Verhaagen, 2006). Of these molecules, tenascin-C is of particular interest. It is thought of as an inhibitory molecule, but it can promote the growth of axons that possess an appropriate tenascin-binding integrin such as α7β1 or α9β1 (Mercado et al., 2004, Andrews et al., 2009). The aim of this study is to use a tenascin-binding integrin to promote spinal cord regeneration.

Integrins are a family of transmembrane cell adhesion receptors possessing an α and a β subunit which can promote neurite outgrowth in embryonic (Lein et al., 1991, Neugebauer et al., 1991), postnatal (Vogelezang et al., 2001) and adult neurons (Condic, 2001, Gardiner et al., 2005, Andrews et al., 2009). Although peripheral nerve regeneration is associated with upregulation of α4, α5, α6, α7 and β1 (Hammarberg et al., 2000, Ekstrom et al., 2003, Vogelezang et al., 2001, Wallquist et al., 2004, Gardiner et al., 2007), α9 integrin which is a receptor for tenascin-

C remains downregulated after CNS injury (Staniszewska et al., 2008, Andrews et al., 2009). The expression of α9 integrin in adult dorsal root ganglion (DRG) neurons promotes profuse sensory axon regeneration *in vitro* on tenascin (Andrews et al., 2009). However the regeneration-promoting effect *in vivo* was modest after spinal cord injury and dorsal root crush. The reason is that integrins are deactivated by the presence of CSPGs and Nogo-A (Tan et al., 2012, Hu and Strittmatter, 2008).

Integrin activation, 'inside-out' signaling, is controlled by the binding of kindlin and talin to the β-integrin cytoplasmic tail (Moser et al., 2009). This enables binding of a ligand to integrin which triggers a series of intracellular signaling cascades, 'outside-in' signaling. The kindlins comprise three isoforms (kindlin-1, -2 and -3) which bind to the β-integrin tail via a FERM (4.1/ezrin/radixin/moesin) domain, triggering activation and cell-matrix adhesion (Rogalski et al., 2000). Kindlin-1 is expressed predominantly in epithelial cells, kindlin-2 is expressed in all tissues and is the only isoform expressed in the nervous system, while kindlin-3 is exclusively expressed in hematopoietic cells (Ussar et al., 2006). Our previous work has demonstrated that expression of kindlin-1, but not kindlin-2, can promote short-distance sensory axon regeneration *in vivo* in the presence of CSPGs (Tan et al., 2012).

The aim of this study was to examine whether the expression of the tenascin-binding α9 integrin with an integrin activator, kindlin-1, could promote extensive sensory axon regeneration in the spinal cord. We have examined sensory axon regeneration *in vitro* and *in vivo* from DRG neurons expressing α9 integrin and kindlin-1 through an environment rich in tenascin-C and CSPGs. We show that activation of α9 integrin by kindlin-1 allows axons to interact with tenascin-C and overcome the inhibitory environment of the adult CNS. Extensive axon

regeneration was observed *in vivo* through a largely normal anatomical pathway with behavioral and physiological restoration of sensory functions. Expression of either α9 integrin or kindlin-1 alone stimulated much less regeneration and recovery.

Materials and Methods

Adult rat DRG cultures

Adult female Sprague-Dawley rats were sacrificed and DRGs were harvested. For explant culture, each DRG was cut into 2-3 pieces and then plated on substrate-coated glass coverslips. For dissociated culture, DRGs were incubated with 0.2% collagenase (Sigma) and 0.1% trypsin (Sigma), followed by trituration and centrifugation. Before being plated on substrate-coated glass coverslips at a density of 2.0-4.0 x 10^4 cells/cm^2, the cells were transfected with Neon transfection kit (Invitrogen). For each reaction, 500 ng of plasmid (α9-eYFP and/or kindlin1-mCherry) was used to transfect 1.0-1.5 x 10^5 cells at 1200 V, 20 ms and 2 pulses. The substrates used for coating were PDL (20 µg/ml, Sigma), laminin (10 µg/ml, Sigma), tenascin-C (10 µg/ml, Millipore) or aggrecan (10 µg/ml, Sigma).

Neurite outgrowth assay

Dissociated cultures were maintained for three days and explant cultures for five days prior to fixation with 4% paraformaldehyde (PFA). Quantification was performed using ImageJ. For dissociated cultures, the longest neurite of 20 randomly-selected DRG neurons per condition was measured (5 independent repeats to give 100 neurons). For explant cultures, the longest 25 neurites per explant per condition were measured (5 explants per condition, 5 independent repeats). To measure the number of neurites extending from each explant, a parallel line was drawn 50 µm away from the edge of the explant, the number of neurites passing through the line was calculated per field of observation (550 µm x 425 µm).

Probe synthesis and in situ hybridization

Probes were synthesized with PCR using the following primers. For α9 integrin, 5'-AGCCGGACGCCAGAGTCCCCT-3' (forward) and 5'-GGAGGGGATGATGTAGCAGAA-3' (reverse). For kindlin-1, 5'-ATGTTCCAGCCTGATCTTTG-3' (forward) and 5'-TGCGAGTTTAGGGATGTCAG-3' (reverse). The purified PCR products were then labelled with digoxigenin (Roche) for *in situ* hybridization on PFA-fixed DRG sections. The procedure for *in situ* hybridization was performed as previously described (Carulli et al., 2006).

Generation of AAV

The plasmids AAV-CMV-fGFP, AAV-CAG-α9-V5, and AAV-CMV-kindlin1-GFP were amplified and sequenced before proceeding to be packaged into AAV5 as described previously (Hermens et al., 1999). For virus production, HEK293T cells were transfected with the individual expression and helper plasmids and kept for three days in culture. The transfected cells were then lysed by using 3 freeze-thaw cycles. After centrifugation, the crude lysate was subjected to iodixanol gradient (15%, 25%, 40% and 60%) ultracentrifugation using a Type 70Ti rotor (Beckman) at 490000 x *g*, 16ºC for 70 min. The virus was then collected and concentrated using an Amicon Ultra-15 device (Millipore). The titer of the virus was then determined by using real-time quantitative PCR - 1.52×10^{13} GC/ml for AAV5-fGFP, 1.54×10^{13} GC/ml for AAV5-α9-V5 and 1.41×10^{13} GC/ml for AAV5-kindlin1-GFP.

Animal surgeries

All animal surgeries were conducted in accordance with the UK Animals (Scientific Procedures) Act 1986. Adult 2-month-old male Lewis rats were used for surgery. Each animal was allocated a number and assigned into one of the control or experimental groups randomly. The experimenter was blinded throughout the entire study including during behavioral testing and axon quantification. During surgery, the animals were anesthetized in 2 - 4% isoflurane, in 1.5 - 2.0 L/min of oxygen. A left hemi-laminectomy was performed at the level C5-T1. 1 µl of the virus at a working titer of 2 x 10^{12} GC/mL was injected into the left C6 and C7 DRG using a 33-gauge needle syringe (Hamilton) with an infusion syringe pump (World Precision Instruments) at 0.1 µl/min, with additional three minutes before needle withdrawal. At the same time, a concurrent dorsal root crush injury (left C5-C8) was performed with a pair of fine Bonn forceps (Fine Science Tools) for 3 x 10 s for each root. A week before the final experimental time point, a total of 5 µl of 1% CTB (List Biological Labs) was injected into the left footpad and the four digits (Carulli et al., 2010). At the end of the experimental time point, the animals were perfused transcardially with 4% PFA. We did not have to humanely kill any animals based on welfare reasons in this study.

Sensory behavioral testing

Ladder rung walking task, mechanical pressure (Randall-Selitto touch sensitivity) test and thermal pain (Hargreave's hotplate) test were administered once before the surgery and once each week after surgery for twelve weeks.

Ladder rung walking task. Animals were placed on a 1.2 m-long horizontal ladder, with uneven spaced rungs which were 3.0 – 5.0 cm apart. Sugar pellets were provided at the end of the

ladder. The animals were allowed to walk on the ladder for three trials and video-recorded. The average number of slips from the three trials was quantified.

Mechanical pressure test. Animals were placed in an enclosure with a metal mesh bottom. A probe connected to an electronic anesthesiometer (IITC Life Science) was applied with a gradual increase of pressure to the footpad of the forepaw, until the animal withdrew its paw. The maximum pressure recorded was termed as the withdrawal force (in grams). Five trials were performed on each forepaw, left (experimental) and right (internal control). The trial was terminated if the animal failed to respond within 100 g. The average withdrawal force was determined after eliminating the highest and lowest measurements.

Thermal test. Animals were placed in an enclosure with a fiberglass bottom. An infrared-emitting device (Ugo Basile) was placed directly under the footpad of the forepaw, until the animal withdrew its paw. The infrared intensity was set at 48 units. The time between the onset of the heat stimulus and withdrawal of the paw was termed as the withdrawal latency (in seconds). Three trials were performed on each forepaw, left (experimental) and right (internal control). The trial was terminated if the animal failed to respond within 20 s. The average withdrawal latency was calculated by averaging the three trials.

Electrophysiology

Animals were terminally anesthetized with urethane (Sigma) at a dosage of 1.5 g/kg. A laminectomy was performed at the level C4-T2. The left dorsal roots C4, C5, C8 and T1 were cut acutely before the recording. The incision cavity was filled with paraffin oil (Sigma). The stimulating electrodes were inserted in parallel into the footpad of the left forepaw (experimental) or right forepaw (internal control). The recording microelectrodes (Platinum/20% Iridium metal, Harvard Apparatus) were inserted into the left and right dorsal horns (≈1 mm

depth), perpendicularly to the spinal cord. The parameters for electrical stimulation were: 4 mA, 100 μs and 5 Hz. The readings were recorded using Spike2 (Cambridge Electronic Design).

Immunostaining

Sections of PFA-fixed tissues were cut at 14 μm on a cryostat. Sections were blocked in 0.4% Triton-X 100 (Sigma) and 10% normal goat serum (Invitrogen). The tissues were then incubated with primary antibodies overnight at 4°C and secondary antibodies for 2 hr at room temperature. After that, the tissues were washed in triplicate of 0.2% Triton-X 100 in PBS and then mounted with Fluorosave (Calbiochem). Primary antibodies used were rabbit anti-β1-integrin (1:500, Millipore), chicken anti-βIII-tubulin (1:500, Abcam), mouse anti-βIII-tubulin (1:500, Sigma), mouse anti-FAK (1:500, Invitrogen), rabbit anti-pY397FAK (1:250, Invitrogen), chicken anti-GFP (1:500, Invitrogen), rabbit anti-GFP (1:1000, Invitrogen), mouse anti-mCherry (1:250, Clontech), mouse anti-V5 (1:250, Invitrogen), mouse anti-chondroitin sulfate (1:400, Sigma), rabbit anti-laminin (1:500, Sigma), rabbit anti-tenascin-C (1:250, Abcam), mouse anti-NF160/200 (1:500, Sigma), mouse anti-NF200 (1:500, Sigma), rabbit anti-CGRP (1:1000, Sigma), biotinylated IB4 (1:500, Vector), goat anti-CTB (1:500, List Biological Labs), guinea pig anti-VGLUT2 (1:500, Synaptic Systems). Secondary antibodies used were Alexa Fluor 488, 568, 647 or 660 (1:500, Invitrogen).

Microscopy and statistical analysis

Fluorescence imaging was performed using a Leica DM6000 epifluorescent microscope and a Leica DMI4000B confocal microscope. Images were analyzed using ImageJ. Bar graphs were shown with mean ± SEM produced using Microsoft Excel 2013. Statistical analysis was performed using SPSS version 22 and statistical differences between groups were determined by using Student's t-test, one-way, two-way or repeated measures ANOVA with Bonferroni

post-hoc test where appropriate. For all statistical analyses, a p value of $p<0.05$ was considered to be significant.

Results

Expression of both α9 integrin and kindlin-1 promotes DRG neurite outgrowth on tenascin-C and aggrecan

To study the independent and synergistic effects of α9 integrin and kindlin-1 *in vitro*, dissociated and explant adult DRG cultures were used to assess neurite outgrowth. Dissociated DRG neurons were transfected with the fusion constructs α9-eYFP and/or kindlin1-mCherry, alongside mock transfected controls. Transfected DRG neurons were cultured on a substrate of laminin (10μg/mL) alone, or tenascin-C (10μg/mL) with or without aggrecan (10μg/mL) for 3 days (Fig. 1A-1C). Due to a lack of commercially reliable antibodies for α9 integrin and kindlin-1, the immunostaining of eYFP was used for detecting α9 integrin and mCherry for kindlin-1. In all cases, βIII tubulin staining was used for neurite length analysis, but α9 integrin and kindlin-1 co-localized with βIII tubulin being present throughout the axons (Fig. 1A). On laminin, the average neurite length was approximately 210 μm for all groups with no statistical differences (Fig. 1B). On tenascin substrates there was almost no growth except from neurons transfected with alpha9 integrin: the alpha9-only (121 ± 30 μm) and alpha9 + kindlin1 (110 ± 34 μm) groups had significantly greater neurite outgrowth (***$p=1.01e^{-5}$, two-way ANOVA, n=5 repeats of 20 neurons each), as compared to the control (32 ± 8 μm) and kindlin1-only (29 ± 9 μm) groups (Fig. 1C). On tenascin-C + aggrecan, the alpha9-only group showed a significant inhibition of neurite outgrowth by aggrecan (**p=0.00274, two-way ANOVA, n=5), 73 ± 18 μm. The alpha9 + kindlin1 group extended long neurites on tenascin-C + aggrecan, 126 ± 30 μm, reversing the inhibitory effect of aggrecan.

To further study the synergistic effect of α9 integrin and kindlin-1, we utilized DRG explant cultures. Specifically, the left C5-C7 DRGs were injected *in vivo* with the viruses AAV5-fGFP,

AAV5-α9-V5 and/or AAV5-kindlin1-GFP four weeks before being harvested for explant culture. The DRG explants were cultured on a substrate of laminin or tenascin-C + aggrecan for 5 days (Fig. 1D-1F). On laminin, the average neurite length was approximately 1000 μm for all groups (Fig. 1E) with an average of 43 neurites per field of observation (Fig. 1F). On tenascin-C + aggrecan, the alpha9 and alpha9 + kindlin1 groups extended significantly longer neurites (***$p=1.76e^{-13}$, one-way ANOVA, n=5) than the fGFP control group (Fig. 1E). The alpha9 + kindlin1 group had the longest average neurite outgrowth (757 ± 221 μm), followed by alpha9-only (584 ± 233 μm), kindlin1-only (224 ± 82 μm) and fGFP (55 ± 21 μm). For the number of neurites per field of observation, the alpha9 + kindlin1 group had 34 ± 10 neurites (***$p=4.77e^{-7}$, one-way ANOVA, n=5), and the alpha9-only group had 15 ± 5 neurites (**p=0.00364, one-way ANOVA, n=5), compared to less than 10 neurites in the kindlin1-only and fGFP groups (Fig. 1F).

Additionally, the overexpression of kindlin-1 increased the phosphorylation of focal adhesion kinase (FAK; *p=0.0108, one-way ANOVA, n=5), demonstrated by an increased immunoreactivity to pY397 FAK in the kindlin1-only (1.2 ± 0.4 unit) and alpha9 + kindlin1 (1.3 ± 0.1 unit) groups (Fig. 2A-2B), indicating downstream signaling cascades triggered by integrin activation (Tan et al., 2011). Collectively, these experiments showed that in both dissociated and explant cultures, α9 integrin expression allowed neurite growth on tenascin-C, but this was inhibited by the presence of aggrecan, confirming our previous results. However, additional expression of kindlin-1 with α9 integrin allowed the neurites to overcome the inhibitory effect of CSPG (aggrecan).

Expression of α9 integrin and kindlin-1 in vivo by adeno-associated virus

Previous studies have shown that adult rat DRG neurons do not express α9 integrin or kindlin-1 (Andrews et al., 2009, Tan et al., 2012, Chiu et al., 2014). In order to express α9 integrin and kindlin-1 ectopically *in vivo* in DRG neurons, we utilized adeno-associated virus serotype 5 (AAV5) for the fusion constructs AAV-CMV-fGFP, AAV-CAG-α9-V5 and AAV-CMV-kindlin1-GFP. As compared to lentivirus and other AAV serotypes (1, 2, 3, 4, 6 and 8), AAV5 has the highest efficiency in transducing DRG neurons over a long time course, up to 12 weeks, when injected directly into the DRG (Mason et al., 2010).

First, we confirmed that our AAVs will co-transduce sensory neurons. Four weeks after direct injection of AAV5-α9-V5 and AAV5-kindlin1-GFP into C6-C7 DRGs, *in situ* hybridization confirmed the positive expression of α9 integrin and kindlin-1 mRNAs, respectively (Fig. 3A). Immunostaining analysis of virus-injected DRG sections showed that AAV5-fGFP had a transduction efficiency of 44 ± 6 %, while AAV5-α9-V5 had a transduction efficiency of 28 ± 3 %, with 33 ± 4 % for AAV5-kindlin1-GFP and 25 ± 6 % for the co-transduction of AAV5-α9-V5 + AAV5-kindlin1-GFP (Fig. 3B-3C). Transduction efficiencies were obtained by measuring the ratio of GFP and/or V5-positive cell bodies with BIII tubulin-positive cell bodies. In addition, further immunostaining showed that AAV5-α9-V5 and AAV5-kindlin1-GFP transduced both large-diameter NF200-positive and small-diameter CGRP-positive DRG neurons (Fig. 3D). Within the DRG and dorsal root, many axons containing both α9 integrin and kindlin-1, visualized by V5 and GFP staining respectively, were seen, and bright kindlin1-GFP-containing axons were clearly seen passing up the spinal cord an innervating the cuneate nucleus, validating it as a good axon tracer equivalent to GFP alone. The staining of α9-V5 was dimmer due to the limitations of the antibody recognizing the short V5 tag, but in most cases axons were seen in the dorsal column up to top of the spinal cord.

Expression of both α9 integrin and kindlin-1 promotes sensory axon regeneration in vivo in a time-dependent manner

AAV5-α9-V5, AAV5-kindlin1-GFP or a combination of the two or AAV5-fGFP control was injected into the left C6 and C7 DRGs at the same time as a concurrent quadruple left C5-C8 dorsal root crush injury in adult rats (4 groups of n=10). Lesions of these four dorsal roots have been demonstrated to be a useful model for forepaw deafferentation (Wu et al., 2009). Twelve weeks after virus injection and injury, axon quantification was performed on the C7 segment of the spinal cord, corresponding to the C7 dermatome map and the area of the forepaw for behavioral testing and electrophysiology (Takahashi and Nakajima, 1996). Depending on which AAV5 the animal had been injected with, the immunostaining of fGFP, the V5 tag on α9 and/or the GFP tag on kindlin-1 was used as a neuronal tracer for axon quantification. In addition, in all animals cholera toxin B subunit (CTB) was injected into the left forepaw as an additional neuronal tracer to ensure that regeneration measures were not confused by the use of different labels, and to confirm for the completeness of dorsal root axotomy through staining of terminals in the cuneate nucleus.

Completeness of dorsal root axotomy

To verify the completeness of axotomy in our crush injury model, we examined the degree of denervation in the spinal cord using electrophysiology and anatomy. A week after dorsal root crush injury, electrophysiological recordings from the dorsal horn in a group of 5 animals showed no compound action potential and no further change was observed when the root was cut subsequently (Fig. 4A). In the main experiment, we used connection to the cuneate nucleus as an indicator of incomplete lesioning. In addition to kindlin-1 which can be observed filling axons and terminals in the cuneate nucleus of animals with no dorsal root injury, we also

utilized CTB for transganglionic tracing of the dorsal column axons (Fig. 4B). This allowed us to further verify the completeness of our crush injury by excluding animals that showed visible CTB and/or kindlin-1 staining in the cuneate nucleus from all anatomical, behavioral and electrophysiological analyses. Using this criteria, from a total of 58 animals that underwent surgery, we excluded 3 animals which showed evidence of incomplete crush injury in the cuneate nucleus.

Regeneration in the dorsal root, DREZ and C7 spinal cord segment

To assess ingrowth into the cord from the virus-injected C7 DRG, we analyzed axon regeneration in the dorsal root, dorsal root entry zone (DREZ) and C7 spinal cord (Fig. 5A). Within the dorsal root, all groups had approximately 47 regenerated axons per 14 μm section (3 sections per animal, n=10) distal to the crush site with no significant difference found between groups (Fig. 5B). Within the DREZ, all three experimental groups, alpha9-only (12 ± 3 axons), kindlin1-only (15 ± 4 axons) and alpha9 + kindlin1 (13 ± 3 axons) showed significantly more axons per 14 μm section (3 sections per animal, *p=0.0466, one-way ANOVA, n=10) than the fGFP control group (2 ± 1 axons) (Fig. 5C). In the C7 spinal cord segment, both the kindlin1-only (22 ± 5 axons) and alpha9 + kindlin1 (48 ± 10 axons) groups had significantly more axons per section (3 sections per animal, ***p=7.99e^{-4}, one-way ANOVA, n=10) than the fGFP control (0.3 ± 0.2 axons) and alpha9-only (2 ± 0.5 axons) groups (Fig. 5D). Furthermore, the alpha9 + kindlin1 group had significantly more axons per section (*p=0.0361, one-way ANOVA, n=10) than the kindlin1-only group. Axons expressing both α9 integrin and kindlin-1 were observed in the spinal cord, especially in the cuneate fasciculus and dorsal horn (Fig. 5E and 5G). For the fGFP control group, no axons were observed growing into the DREZ and spinal cord (Fig. 5F).

Long-distance regeneration in the spinal cord with dual expression of α9 integrin and kindlin-1

For animals treated with both α9 integrin and kindlin-1, further assessment along the spinal cord revealed regenerated axons in the dorsal column all the way up to level C1 and medulla with no kindlin-1 or CTB immunopositive axons observed in the cuneate nucleus (Fig. 6A). However, only a limited amount of regeneration with less than a spinal segment was observed in animals treated with α9 integrin only (Fig. 6B). The long-distance regeneration with a maximum axon length averaged between animals of 25 ± 3 mm observed in the alpha9 + kindlin1 group was highly significant (***$p=1.66e^{-10}$, one-way ANOVA, n=5) as compared to the fGFP, alpha9-only and kindlin1-only groups in which only a segment or less (≤4 mm) regeneration was observed (Fig. 6C). In the alpha9 + kindlin1 group at C5/C6 segment, an average of 31 axons per section was counted while at C3/C4 and C1/C2 segments there was still a robust projection with approximately 10 axons per section (Fig. 6D).

Additionally, further assessment of those regenerated axons revealed that a proportion of the regenerated kindlin1-positive axons were NF200, CGRP- and IB4-immunopositive (Fig. 7A). Many NF200-immunopositive axons were observed as axons of passage in the cuneate fasciculus of the dorsal column. Within the dorsal horn we counted the proportion of kindlin-1-positive regenerated processes that stained for the three markers. NF200 processes were 17 ± 6 % in laminae I-II (substantia gelatinosa), 59 ± 8 % in the deeper laminae III-V (nucleus proprius) of the dorsal horn. CGRP processes were 44 ± 10 % in laminae I-II, 21 ± 7 % in laminae III-V, and IB4-immunopositive processes were 32 ± 8 % in laminae 1-II, 14 ± 4 % in

laminae III-V. The innervation pattern of axonal subtypes was similar to normal spinal cord but less precise (Fig. 7B). Using confocal microscopy of single optical slices, kindlin-1-expressing sensory axon terminals were observed in the dorsal horn to be co-localized with the VGlut2 puncta of dorsal horn neurons, indicating potential synaptic reconnections (Fig. 7C). Together, these data show that axons expressing both α9 integrin and kindlin-1 are able to regenerate through the DREZ, where they follow appropriate pathways and terminal zones within the spinal cord, and within 12 weeks they can grow for up to 7 spinal segments and over 25 mm in length.

Time course of regeneration

For the alpha9 + kindlin1 group, we further assessed axon regeneration at 3 and 6 week time-points in an additional set of animals (2 groups of n=5) (Fig. 8A). At 3 weeks (which is the time it takes for maximal AAV-driven expression to build up), regenerating axons were observed in the dorsal root (27 ± 5 axons per section, 3 sections per animal, n=5), with a few in the DREZ (3 ± 1 axons, 3 sections per animal, n=5) and none were found in the spinal cord (Fig. 8B). At 6 weeks, significantly more regenerating axons were observed in the DREZ (14 ± 3 axons per section, 3 sections per animal, *p=0.0414, Student's t-test, n=5) and spinal cord (25 ± 4 axons per section, 3 sections per animal, **p=0.00951, Student's t-test, n=5). Taken together with the data obtained at the 12 week time-point, these data demonstrate that expression of both α9 integrin and kindlin-1 significantly promotes sensory axon regeneration in a time-dependent manner because the level of regeneration was observed to increase over time from 3 to 6 to 12 weeks.

Changes in extracellular matrix molecules in the DREZ

For this study, the DREZ was defined as the segment in the dorsal root which was immunonegative for laminin (Fig. 9A). Laminin was highly expressed in the dorsal root, but not in the DREZ central to where the dorsal root joins the spinal cord. Additionally, the immunoreactivity of laminin does not change in the DREZ after injury (McPhail et al., 2007), hence the staining of laminin is a good delineator between the PNS and CNS environments of the dorsal root. Twelve weeks after dorsal root crush injury, there was an upregulation of CSPGs in the injured dorsal root and of tenascin-C in the DREZ (Fig. 9B). A dorsal root crush did not upregulate the expression of CSPGs and tenascin-C in the contralateral uninjured dorsal root (Fig. 9B). Axons in the fGFP control group did not grow into the tenascin-C-rich DREZ while axons expressing both α9 integrin and kindlin-1 were observed growing beyond the tenascin-C-rich DREZ and into the spinal cord (Fig. 9C). This is consistent with our *in vitro* experiments, with tenascin-C in the DREZ being inhibitory to sensory axon regeneration. However, for axons expressing α9 integrin, this tenascin-C would be a growth-promoting substrate.

Treatment with α9 integrin and kindlin-1 promotes electrophysiological reconnection

To further investigate functional sensory axon regeneration, electrophysiological recording was performed at the end of the 12 week experimental time-point. The left dorsal roots C4, C5, C8 and T1 were cut acutely to eliminate spinal inputs from overlapping dermatomes while leaving C7 intact. Extracellular platinum-iridium recording electrodes were inserted into the left and right C7 dorsal horns. At the 12 week time-point, there were large differences in the size of the dorsal column compound action potentials recorded from the control and three experimental groups (alpha9-only, kindlin1-only and alpha9 + kindlin1) (Fig. 10A). In all cases,

when the C7 dorsal root was cut subsequently during the recording session, the compound action potential was completely eliminated. We saw no evidence of reconnection in the fGFP control group. As compared to the fGFP control group (3 ± 0.2 μV), the alpha9 + kindlin1 group showed the highest peak-to-peak voltage amplitude of 64 ± 20 μV (**p=0.00352, one-way ANOVA, n=5), followed by the alpha9-only (21 ± 5 μV) and kindlin1-only (21 ± 1 μV) groups (*p=0.0266, one-way ANOVA, n=5) (Fig. 10B). This was compared with an amplitude of 159 ± 20 μV in uninjured controls.

Treatment with α9 integrin and kindlin-1 promotes sensory-motor behavioral recovery

To examine sensory behavioral recovery, mechanical pressure (Randall-Selitto touch sensitivity) test, thermal pain (Hargreave's hotplate) test and uneven-rung ladder-walking task were administered up to a week before the surgery with pre-training on the ladder, and then weekly after surgery for 12 weeks. A week after surgery, the experimental left forepaw from all groups showed significant sensory deficits in all three behavioral tests as compared to pre-surgery levels (Fig. 11A-11C). This was indicated by a higher withdrawal force and a longer withdrawal time was required to initiate paw withdrawal, and an almost complete inability to place the left forepaw on the rungs during the ladder-walking task.

In the mechanical pressure test, the alpha9 + kindlin1 group started to show a significant recovery (**p=0.00926, repeated measures ANOVA, n=10) from week 8 while the other three groups, fGFP control, alpha9-only and kindlin1-only, did not show any significant recovery (Fig. 11A). In the thermal test, all three experimental groups (alpha9-only, kindlin1-only and alpha9 + kindlin1) showed a significant recovery (*p=0.0271, repeated measures ANOVA,

n=10 per group) as compared to the fGFP control group (Fig. 11B). The alpha9 + kindlin1 group showed a faster and more significant recovery at an earlier time-point (week 5) as compared to the kindlin1-only (week 7) and alpha9-only (week 8) groups. In the ladder-walking task, the control group showed very inaccurate limb placement throughout. The alpha9 + kindlin1 group showed significant recovery in limb proprioception (**p=0.00631, repeated measures ANOVA, n=10) from week 9 and the kindlin1-only group possibly showed marginal recovery from week 11 (*p=0.0429, repeated measures ANOVA, n=10), but the fGFP control and alpha9-only groups did not recover (Fig. 11C). Taken together, these results indicate that the alpha9 + kindlin1 group showed excellent sensory recovery in the mechanical pressure and thermal tests, and excellent sensory-motor recovery in the ladder-walking task. The kindlin1-only group showed a delayed recovery in the thermal and possibly ladder-walking tests, while the alpha9-only group showed recovery only in the thermal test, while the fGFP control group showed no recovery in any test.

Discussion

This study demonstrates that sensory axons are able to regenerate for substantial distances following a dorsal root axotomy provided that they have on their surface an integrin co-expressed with an inside-out activator, kindlin-1. Alpha9 integrin binds to tenascin-C, a constituent of the non-permissive environment in the adult spinal cord, and kindlin-1 prevents it from being deactivated by CSPGs. Our previous studies (Andrews et al., 2009, Tan et al., 2012) had shown that expression of either α9 integrin or kindlin-1 in DRG neurons could enhance regeneration of axons into the spinal cord through the DREZ, but there was little growth from this point of entry along the length of the cord. In this study we show that the combinatorial expression of α9 integrin and kindlin-1 promotes axon regeneration over remarkably long distances, 25 mm or seven spinal levels and more, all the way up to the medulla. The regenerating axons follow a relatively normal pathway, re-form synaptic connections in appropriate regions of the dorsal horn, and can re-establish sensory and sensory-motor behaviors. While the combination of α9 integrin and kindlin-1 enabled useful reconstruction of sensory connections and function, our results with α9 integrin alone or kindlin-1 alone confirm our previous studies, promoting regeneration for 4 mm or less with only recovery of heat sensation.

Expression and activation of an appropriate integrin

Axons will not grow unless they have on their surface a receptor that recognizes a ligand in their environment. Our previous work has identified α9 integrin as such a receptor, recognizing tenascin-C which is present in the DREZ and CNS environment. However axon regeneration *in vivo* after expression of this integrin was modest (Andrews et al., 2009). The probable reason for the limited effect of α9 integrin *in vivo* is that it is inactivated by CSPGs and Nogo-A found

in the injured CNS (Hu and Strittmatter, 2008, Tan et al., 2012). The signaling pathway is not identified, but intracellularly, the Rho/ROCK pathway has been suggested to mediate the growth inhibition of CSPGs (Monnier et al., 2003) and myelin-associated inhibitors (Niederost et al., 2002), and integrin-mediated suppression of the Rho/ROCK pathway is required to promote cell motility (Arthur et al., 2000). Additionally, kindlin-1 (Tan et al., 2012) and full-length talin (Tan et al., 2015) have been shown to promote neurite outgrowth in the presence of CSPGs by binding to β1 integrin for integrin activation, resulting in increased integrin signaling via focal adhesion kinase (FAK) and integrin linked kinase (ILK) (Schaller et al., 1995, Novak et al., 1998). Kindlins activate integrins by binding to the beta tail via their FERM domain. They also bind to PIP3 and paxillin (Theodosiou et al., 2016, Rognoni et al., 2016). Full-length talin cannot be used for promoting neuronal regeneration because of its large size, and the talin head which contains the integrin-binding and activating site inhibits axon growth, probably by competing with full-length talin (Tan et al., 2015).

In the present experiments, we have expressed α9 integrin which combines with the pool of β1 subunit in adult DRG neurons to produce α9β1 integrin, which can then be activated via the inside-out pathway using kindlin-1. Tissue culture experiments using dissociated adult DRG neurons and adult DRGs transduced *in vivo* showed that α9β1 integrin promotes growth on tenascin-C, but this growth is inhibited by CSPGs. Activation with kindlin-1 enables the axons to overcome this CSPG inhibition. The same combination of molecules was then transduced into DRG neurons *in vivo* coupled with dorsal root crush injury. Axons expressing either α9 integrin or kindlin-1 alone showed limited regeneration through the DREZ into the cord, but only the synergistic effect of α9 integrin and kindlin-1 co-expression resulted in a combined effect which led to much greater axon regeneration, with many axons regenerating 7 or more spinal levels to and beyond C1, for a length of up to 25 mm and above. It will be important to

study the regenerative effect of α9 integrin and kindlin-1 co-expression when the injury is placed in the spinal cord rather than the dorsal root. Tenascin-C is strongly upregulated around spinal injuries, so it is probable that axons expressing activated α9 integrin will grow extensively in this environment, as they did through the upregulated tenascin-C at the DREZ in the present study.

It is interesting that kindlin-1-only expressing axons were able to grow a limited distance into the spinal cord, while kindlin-1 did not increase growth in our *in vitro* experiments. We assume that this occurs because DRGs express various integrins such as αVβ8 and α7β1 (Tucker and Chiquet-Ehrismann, 2015, Chiu et al., 2014), which become activated allowing them to interact with various integrin ligands in the spinal cord, whereas in the *in vitro* assay only tenascin-C and aggrecan were present. These kindlin-1-activated integrins were able to produce some axon growth, but were relatively ineffective compared to activated α9β1 integrin.

Long-distance axon regeneration in the spinal cord

We have demonstrated complete axotomy electrophysiologically and by using two tracers to demonstrate complete denervation of the cuneate nucleus; this was a good control because no axons regenerated back to the cuneate nucleus. We also examined the time course of regeneration, finding regeneration into the DREZ at 3 weeks, to the lower cervical cord at 6 weeks, and to C1 and above at 12 weeks. To date, dorsal column regeneration to the nucleus has only been reported in cases with high cervical lesion and with neurotrophin stimulation (Alto et al., 2009, Bonner et al., 2011) or at a longer experimental time-point of up to 6 months after treatment with artemin (Wang et al., 2008, Wong et al., 2015). Combinatorial overexpression of two neuronal intrinsic regeneration-associated genes, GAP43 and CAP23

(Bomze et al., 2001), or four regeneration-associated transcription factors, ATF3, c-Jun, STAT3 and Smad1 (Fagoe et al., 2015) have produced relatively modest sensory axon regeneration. The current approach of combining an integrin with an integrin activator seems to be the most effective strategy to boost the intrinsic regenerative capacity of an injured sensory neuron.

The pathway taken by the regenerating axons was remarkably normal, with most NF200-positive axons travelling in the dorsal column and re-innervation of the dorsal horn by NF200-, CGRP- and IB4-positive processes being mainly in the correct layers, although less precise than normal. This implies either that some axon guidance information remains in the denervated adult cord, and/or that the axons were following the physical pathways of the degenerated axons. We did not see evidence of axonal misguidance or wandering as observed in some recent regeneration experiments (Luo et al., 2013). We suggest that stimulation of regeneration through expression of an appropriate surface receptor allows for normal signaling within the axons, while maximal direct activation of signaling pathways might render axons dazzled and unable to see features in their environment.

Behavioral recovery

Animals receiving treatment of both α9 integrin and kindlin-1 showed good recovery in all three behavioral tests despite no direct re-innervation of the cuneate nucleus. The observation that thermal pain sensation is restored even with the very limited and local re-innervation that we saw in the α9 integrin or kindlin-1 alone groups is consistent with the view that heat withdrawal is a local spinal reflex. However mechanical pressure sensation and ladder-walking proprioception were restored only in those animals treated with both α9 integrin and kindlin-1,

suggesting that a more complete re-innervation is required for these behaviors. Although there was no direct re-innervation of the cuneate nucleus, it is possible that propriospinal neurons received input from regenerated axons and then relayed information up to the brain.

The prolific regeneration that we have seen in sensory axons forced to express α9 integrin and kindlin-1 begs the question of whether this strategy could be used to promote regeneration of intrinsic CNS axons. However, there are problems with this approach. Integrins are transported readily down adult DRG neurons to be inserted into the growth cones (Eva et al., 2012, Eva et al., 2010), explaining how α9 integrin expression can promote dorsal column regeneration. However trafficking of integrins in cortical neuron axons is very different. During developmental growth, cortical neurons transport integrins, but with neuronal maturity integrins become restricted to the somatodendritic domain and are excluded from the axons, hence contributing to the developmental loss of regenerative ability in CNS axons (Franssen et al., 2015, Heintz et al., 2014). Extension of the α9 integrin-kindlin-1 approach to CNS axons will require a solution to this issue. However it is now reasonable to ask whether it would be possible to restore useful sensation to patients with spinal injuries. Restoration of sensation would enable patients to avoid burns, pressure sores and other damage and to improve manipulative ability. In addition, restoration of genital sensation is a desired outcome for many patients (Anderson, 2004).

References

ALTO, L. T., HAVTON, L. A., CONNER, J. M., HOLLIS, E. R., 2ND, BLESCH, A. & TUSZYNSKI, M. H. 2009. Chemotropic guidance facilitates axonal regeneration and synapse formation after spinal cord injury. *Nat Neurosci,* 12**,** 1106-13.

ANDERSON, K. D. 2004. Targeting recovery: priorities of the spinal cord-injured population. *J. Neurotrauma,* 21**,** 1371-1383.

ANDREWS, M. R., CZVITKOVICH, S., DASSIE, E., VOGELAAR, C. F., FAISSNER, A., BLITS, B., GAGE, F. H., FFRENCH-CONSTANT, C. & FAWCETT, J. W. 2009. Alpha9 integrin promotes neurite outgrowth on tenascin-C and enhances sensory axon regeneration. *J Neurosci,* 29**,** 5546-57.

ARTHUR, W. T., PETCH, L. A. & BURRIDGE, K. 2000. Integrin engagement suppresses RhoA activity via a c-Src-dependent mechanism. *Curr Biol,* 10**,** 719-22.

BOMZE, H. M., BULSARA, K. R., ISKANDAR, B. J., CARONI, P. & SKENE, J. H. 2001. Spinal axon regeneration evoked by replacing two growth cone proteins in adult neurons. *Nat Neurosci,* 4**,** 38-43.

BONNER, J. F., CONNORS, T. M., SILVERMAN, W. F., KOWALSKI, D. P., LEMAY, M. A. & FISCHER, I. 2011. Grafted neural progenitors integrate and restore synaptic connectivity across the injured spinal cord. *J Neurosci,* 31**,** 4675-86.

BRADBURY, E. J., MOON, L. D., POPAT, R. J., KING, V. R., BENNETT, G. S., PATEL, P. N., FAWCETT, J. W. & MCMAHON, S. B. 2002. Chondroitinase ABC promotes functional recovery after spinal cord injury. *Nature,* 416**,** 636-40.

CAFFERTY, W. B., YANG, S. H., DUFFY, P. J., LI, S. & STRITTMATTER, S. M. 2007. Functional axonal regeneration through astrocytic scar genetically modified to digest chondroitin sulfate proteoglycans. *J Neurosci,* 27**,** 2176-85.

CARULLI, D., PIZZORUSSO, T., KWOK, J. C., PUTIGNANO, E., POLI, A., FOROSTYAK, S., ANDREWS, M. R., DEEPA, S. S., GLANT, T. T. & FAWCETT, J. W. 2010. Animals lacking link protein have attenuated perineuronal nets and persistent plasticity. *Brain,* 133**,** 2331-47.

CARULLI, D., RHODES, K. E., BROWN, D. J., BONNERT, T. P., POLLACK, S. J., OLIVER, K., STRATA, P. & FAWCETT, J. W. 2006. Composition of perineuronal nets in the adult rat cerebellum and the cellular origin of their components. *J Comp Neurol,* 494**,** 559-77.

CHIU, I. M., BARRETT, L. B., WILLIAMS, E. K., STROCHLIC, D. E., LEE, S., WEYER, A. D., LOU, S., BRYMAN, G. S., ROBERSON, D. P., GHASEMLOU, N., PICCOLI, C., AHAT, E., WANG, V., COBOS, E. J., STUCKY, C. L., MA, Q., LIBERLES, S. D. & WOOLF, C. J. 2014. Transcriptional profiling at whole population and single cell levels reveals somatosensory neuron molecular diversity. *Elife,* 3.

CONDIC, M. L. 2001. Adult neuronal regeneration induced by transgenic integrin expression. *J Neurosci,* 21**,** 4782-8.

EKSTROM, P. A., MAYER, U., PANJWANI, A., POUNTNEY, D., PIZZEY, J. & TONGE, D. A. 2003. Involvement of alpha7beta1 integrin in the conditioning-lesion effect on sensory axon regeneration. *Mol Cell Neurosci,* 22**,** 383-95.

EVA, R., CRISP, S., MARLAND, J. R., NORMAN, J. C., KANAMARLAPUDI, V., FFRENCH-CONSTANT, C. & FAWCETT, J. W. 2012. ARF6 Directs Axon Transport and Traffic of Integrins and Regulates Axon Growth in Adult DRG Neurons. *J. Neurosci,* 32**,** 10352-10364.

EVA, R., DASSIE, E., CASWELL, P. T., DICK, G., FFRENCH-CONSTANT, C., NORMAN, J. C. & FAWCETT, J. W. 2010. Rab11 and Its Effector Rab Coupling Protein Contribute to the Trafficking of {beta}1 Integrins during Axon Growth in Adult Dorsal Root Ganglion Neurons and PC12 Cells. *J. Neurosci,* 30**,** 11654-11669.

FAGOE, N. D., ATTWELL, C. L., KOUWENHOVEN, D., VERHAAGEN, J. & MASON, M. R. 2015. Overexpression of ATF3 or the combination of ATF3, c-Jun, STAT3 and Smad1 promotes regeneration of the central axon branch of sensory neurons but without synergistic effects. *Hum Mol Genet,* 24**,** 6788-800.

FRANSSEN, E. H., ZHAO, R. R., KOSEKI, H., KANAMARLAPUDI, V., HOOGENRAAD, C. C., EVA, R. & FAWCETT, J. W. 2015. Exclusion of integrins from CNS axons is regulated by Arf6 activation and the AIS. *J Neurosci,* 35**,** 8359-75.

FRIEDLANDER, D. R., MILEV, P., KARTHIKEYAN, L., MARGOLIS, R. K., MARGOLIS, R. U. & GRUMET, M. 1994. The neuronal chondroitin sulfate proteoglycan neurocan binds to the neural cell adhesion molecules Ng-CAM/L1/NILE and N-CAM, and inhibits neuronal adhesion and neurite outgrowth. *J Cell Biol,* 125**,** 669-80.

GARDINER, N. J., FERNYHOUGH, P., TOMLINSON, D. R., MAYER, U., VON DER MARK, H. & STREULI, C. H. 2005. Alpha7 integrin mediates neurite outgrowth of distinct populations of adult sensory neurons. *Mol Cell Neurosci,* 28**,** 229-40.

GARDINER, N. J., MOFFATT, S., FERNYHOUGH, P., HUMPHRIES, M. J., STREULI, C. H. & TOMLINSON, D. R. 2007. Preconditioning injury-induced neurite outgrowth of

adult rat sensory neurons on fibronectin is mediated by mobilisation of axonal alpha5 integrin. *Mol Cell Neurosci,* 35**,** 249-60.

HAMMARBERG, H., WALLQUIST, W., PIEHL, F., RISLING, M. & CULLHEIM, S. 2000. Regulation of laminin-associated integrin subunit mRNAs in rat spinal motoneurons during postnatal development and after axonal injury. *J Comp Neurol,* 428**,** 294-304.

HEINTZ, T. G., HELLER, J. P., ZHAO, R., CACERES, A., EVA, R. & FAWCETT, J. W. 2014. Kinesin KIF4A transports integrin beta1 in developing axons of cortical neurons. *Mol Cell Neurosci,* 63**,** 60-71.

HERMENS, W. T., TER BRAKE, O., DIJKHUIZEN, P. A., SONNEMANS, M. A., GRIMM, D., KLEINSCHMIDT, J. A. & VERHAAGEN, J. 1999. Purification of recombinant adeno-associated virus by iodixanol gradient ultracentrifugation allows rapid and reproducible preparation of vector stocks for gene transfer in the nervous system. *Hum Gene Ther,* 10**,** 1885-91.

HU, F. & STRITTMATTER, S. M. 2008. The N-terminal domain of Nogo-A inhibits cell adhesion and axonal outgrowth by an integrin-specific mechanism. *J Neurosci,* 28**,** 1262-9.

JOESTER, A. & FAISSNER, A. 1999. Evidence for combinatorial variability of tenascin-C isoforms and developmental regulation in the mouse central nervous system. *J Biol Chem,* 274**,** 17144-51.

KWOK, J. C., YANG, S. & FAWCETT, J. W. 2014. Neural ECM in regeneration and rehabilitation. *Prog Brain Res,* 214**,** 179-92.

LEIN, P. J., HIGGINS, D., TURNER, D. C., FLIER, L. A. & TERRANOVA, V. P. 1991. The NC1 domain of type IV collagen promotes axonal growth in sympathetic neurons through interaction with the alpha 1 beta 1 integrin. *J Cell Biol,* 113**,** 417-28.

LUNDELL, A., OLIN, A. I., MORGELIN, M., AL-KARADAGHI, S., ASPBERG, A. & LOGAN, D. T. 2004. Structural basis for interactions between tenascins and lectican C-type lectin domains: evidence for a crosslinking role for tenascins. *Structure,* 12**,** 1495-506.

LUO, X., SALGUEIRO, Y., BECKERMAN, S. R., LEMMON, V. P., TSOULFAS, P. & PARK, K. K. 2013. Three-dimensional evaluation of retinal ganglion cell axon regeneration and pathfinding in whole mouse tissue after injury. *Exp Neurol,* 247**,** 653-62.

MASON, M. R., EHLERT, E. M., EGGERS, R., POOL, C. W., HERMENING, S., HUSEINOVIC, A., TIMMERMANS, E., BLITS, B. & VERHAAGEN, J. 2010.

Comparison of AAV serotypes for gene delivery to dorsal root ganglion neurons. *Mol Ther,* 18**,** 715-24.

MCPHAIL, L. T., BORISOFF, J. F., TSANG, B., HWI, L. P., KWIECIEN, J. M. & RAMER, M. S. 2007. Protracted myelin clearance hinders central primary afferent regeneration following dorsal rhizotomy and delayed neurotrophin-3 treatment. *Neurosci Lett,* 411**,** 206-11.

MERCADO, M. L., NUR-E-KAMAL, A., LIU, H. Y., GROSS, S. R., MOVAHED, R. & MEINERS, S. 2004. Neurite outgrowth by the alternatively spliced region of human tenascin-C is mediated by neuronal alpha7beta1 integrin. *J Neurosci,* 24**,** 238-47.

MILEV, P., FISCHER, D., HARING, M., SCHULTHESS, T., MARGOLIS, R. K., CHIQUET-EHRISMANN, R. & MARGOLIS, R. U. 1997. The fibrinogen-like globe of tenascin-C mediates its interactions with neurocan and phosphacan/protein-tyrosine phosphatase-zeta/beta. *J Biol Chem,* 272**,** 15501-9.

MONNIER, P. P., SIERRA, A., SCHWAB, J. M., HENKE-FAHLE, S. & MUELLER, B. K. 2003. The Rho/ROCK pathway mediates neurite growth-inhibitory activity associated with the chondroitin sulfate proteoglycans of the CNS glial scar. *Mol Cell Neurosci,* 22**,** 319-30.

MOON, L. D., ASHER, R. A., RHODES, K. E. & FAWCETT, J. W. 2001. Regeneration of CNS axons back to their target following treatment of adult rat brain with chondroitinase ABC. *Nat Neurosci,* 4**,** 465-6.

MOSER, M., LEGATE, K. R., ZENT, R. & FASSLER, R. 2009. The tail of integrins, talin, and kindlins. *Science,* 324**,** 895-9.

NEUGEBAUER, K. M., EMMETT, C. J., VENSTROM, K. A. & REICHARDT, L. F. 1991. Vitronectin and thrombospondin promote retinal neurite outgrowth: developmental regulation and role of integrins. *Neuron,* 6**,** 345-58.

NIEDEROST, B., OERTLE, T., FRITSCHE, J., MCKINNEY, R. A. & BANDTLOW, C. E. 2002. Nogo-A and myelin-associated glycoprotein mediate neurite growth inhibition by antagonistic regulation of RhoA and Rac1. *J Neurosci,* 22**,** 10368-76.

NOVAK, A., HSU, S. C., LEUNG-HAGESTEIJN, C., RADEVA, G., PAPKOFF, J., MONTESANO, R., ROSKELLEY, C., GROSSCHEDL, R. & DEDHAR, S. 1998. Cell adhesion and the integrin-linked kinase regulate the LEF-1 and beta-catenin signaling pathways. *Proc Natl Acad Sci U S A,* 95**,** 4374-9.

PASTERKAMP, R. J. & VERHAAGEN, J. 2006. Semaphorins in axon regeneration: developmental guidance molecules gone wrong? *Philos Trans R Soc Lond B Biol Sci,* 361**,** 1499-511.

PROBSTMEIER, R., BRAUNEWELL, K. & PESHEVA, P. 2000. Involvement of chondroitin sulfates on brain-derived tenascin-R in carbohydrate-dependent interactions with fibronectin and tenascin-C. *Brain Res,* 863**,** 42-51.

PROBSTMEIER, R. & PESHEVA, P. 1999. Tenascin-C inhibits beta1 integrin-dependent cell adhesion and neurite outgrowth on fibronectin by a disialoganglioside-mediated signaling mechanism. *Glycobiology,* 9**,** 101-14.

ROGALSKI, T. M., MULLEN, G. P., GILBERT, M. M., WILLIAMS, B. D. & MOERMAN, D. G. 2000. The UNC-112 gene in Caenorhabditis elegans encodes a novel component of cell-matrix adhesion structures required for integrin localization in the muscle cell membrane. *J Cell Biol,* 150**,** 253-64.

ROGNONI, E., RUPPERT, R. & FASSLER, R. 2016. The kindlin family: functions, signaling properties and implications for human disease. *J Cell Sci,* 129**,** 17-27.

SCHALLER, M. D., OTEY, C. A., HILDEBRAND, J. D. & PARSONS, J. T. 1995. Focal adhesion kinase and paxillin bind to peptides mimicking beta integrin cytoplasmic domains. *J Cell Biol,* 130**,** 1181-7.

STANISZEWSKA, I., SARIYER, I. K., LECHT, S., BROWN, M. C., WALSH, E. M., TUSZYNSKI, G. P., SAFAK, M., LAZAROVICI, P. & MARCINKIEWICZ, C. 2008. Integrin alpha9 beta1 is a receptor for nerve growth factor and other neurotrophins. *J Cell Sci,* 121**,** 504-13.

TAKAHASHI, Y. & NAKAJIMA, Y. 1996. Dermatomes in the rat limbs as determined by antidromic stimulation of sensory C-fibers in spinal nerves. *Pain,* 67**,** 197-202.

TAN, C. L., ANDREWS, M. R., KWOK, J. C., HEINTZ, T. G., GUMY, L. F., FASSLER, R. & FAWCETT, J. W. 2012. Kindlin-1 enhances axon growth on inhibitory chondroitin sulfate proteoglycans and promotes sensory axon regeneration. *J Neurosci,* 32**,** 7325-35.

TAN, C. L., KWOK, J. C., HELLER, J. P., ZHAO, R., EVA, R. & FAWCETT, J. W. 2015. Full length talin stimulates integrin activation and axon regeneration. *Mol Cell Neurosci,* 68**,** 1-8.

TAN, C. L., KWOK, J. C., PATANI, R., FFRENCH-CONSTANT, C., CHANDRAN, S. & FAWCETT, J. W. 2011. Integrin activation promotes axon growth on inhibitory

chondroitin sulfate proteoglycans by enhancing integrin signaling. *J Neurosci,* 31**,** 6289-95.

THEODOSIOU, M., WIDMAIER, M., BOTTCHER, R. T., ROGNONI, E., VEELDERS, M., BHARADWAJ, M., LAMBACHER, A., AUSTEN, K., MULLER, D. J., ZENT, R. & FASSLER, R. 2016. Kindlin-2 cooperates with talin to activate integrins and induces cell spreading by directly binding paxillin. *Elife,* 5.

TUCKER, R. P. & CHIQUET-EHRISMANN, R. 2015. Tenascin-C: Its functions as an integrin ligand. *Int J Biochem Cell Biol,* 65**,** 165-8.

USSAR, S., WANG, H. V., LINDER, S., FASSLER, R. & MOSER, M. 2006. The Kindlins: subcellular localization and expression during murine development. *Exp Cell Res,* 312**,** 3142-51.

VOGELEZANG, M. G., LIU, Z., RELVAS, J. B., RAIVICH, G., SCHERER, S. S. & FFRENCH-CONSTANT, C. 2001. Alpha4 integrin is expressed during peripheral nerve regeneration and enhances neurite outgrowth. *J Neurosci,* 21**,** 6732-44.

WALLQUIST, W., ZELANO, J., PLANTMAN, S., KAUFMAN, S. J., CULLHEIM, S. & HAMMARBERG, H. 2004. Dorsal root ganglion neurons up-regulate the expression of laminin-associated integrins after peripheral but not central axotomy. *J Comp Neurol,* 480**,** 162-9.

WANG, R., KING, T., OSSIPOV, M. H., ROSSOMANDO, A. J., VANDERAH, T. W., HARVEY, P., CARIANI, P., FRANK, E., SAH, D. W. & PORRECA, F. 2008. Persistent restoration of sensory function by immediate or delayed systemic artemin after dorsal root injury. *Nat Neurosci,* 11**,** 488-96.

WONG, L. E., GIBSON, M. E., ARNOLD, H. M., PEPINSKY, B. & FRANK, E. 2015. Artemin promotes functional long-distance axonal regeneration to the brainstem after dorsal root crush. *Proc Natl Acad Sci U S A,* 112**,** 6170-5.

WU, A., LAUSCHKE, J. L., MORRIS, R. & WAITE, P. M. 2009. Characterization of rat forepaw function in two models of cervical dorsal root injury. *J Neurotrauma,* 26**,** 17-29.

Figures & Legends

Figure 1

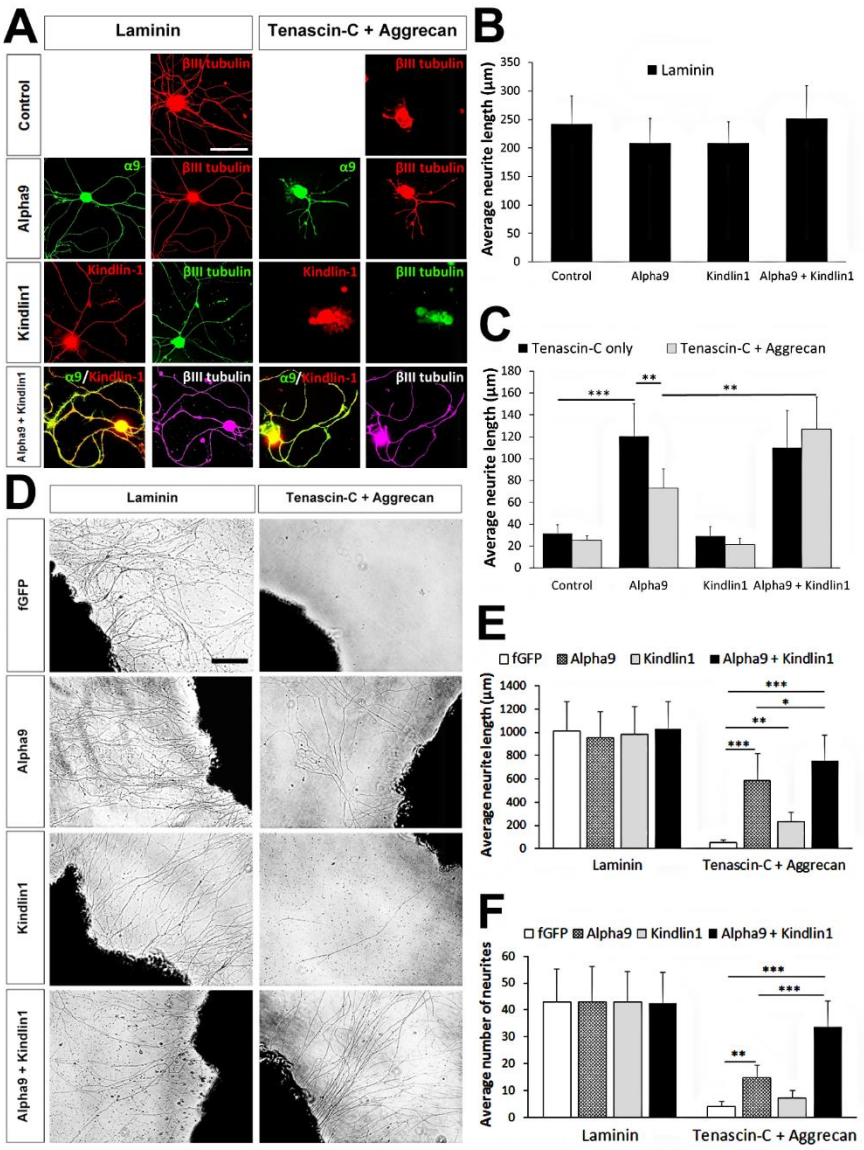

Figure 1. Co-expression of α9 integrin and kindlin-1 promotes DRG neurite outgrowth *in vitro* on tenascin-C + aggrecan

(A) Neurite outgrowth of dissociated DRG neurons, mock transfected (control) or transfected with α9-eYFP and/or kindlin1-mCherry cultured on laminin or tenascin-C + aggrecan. Scale bar is 100 µm. **(B-C)** The average neurite length of dissociated DRG neurons cultured on laminin (**B**), tenascin-C only or tenascin-C + aggrecan (**C**) for 3 days, n=5. **(D)** Neurite outgrowth of DRG explants injected with AAV5-fGFP, AAV5-α9-V5 and/or AAV5-kindlin1-GFP cultured on laminin or tenascin-C + aggrecan. Scale bar is 100 µm. **(E-F)** The average neurite length (**E**) and the average number of neurites per field of observation (**F**) of virus-injected DRG explants cultured on laminin or tenascin-C + aggrecan for 5 days, n=5. Results were analyzed by one-way (**B**, **E**, **F**) or two-way (**C**) ANOVA and expressed as mean ± SEM, *p<0.05, **p<0.01 and ***p<0.001 were statistically significant.

Figure 2

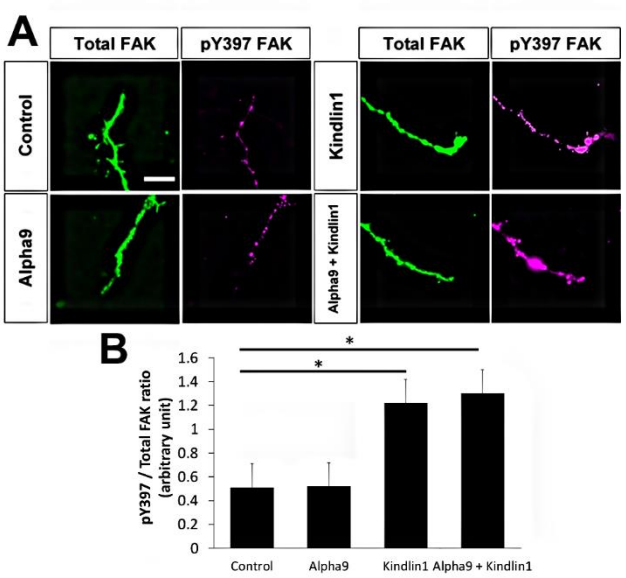

Figure 2. Overexpression of kindlin-1 increases phosphorylation of FAK

(A) DRG neurons, mock transfected (control) or transfected with α9-eYFP and/or kindlin1-mCherry cultured on laminin, labeled with antibodies to FAK and pY397 FAK. Scale bar is 30 μm. **(B)** Quantification of pY397 / total FAK ratio in arbitrary unit, analyzed by one-way ANOVA and expressed as mean ± SEM, *$p<0.05$ was statistically significant, n=5.

Figure 3

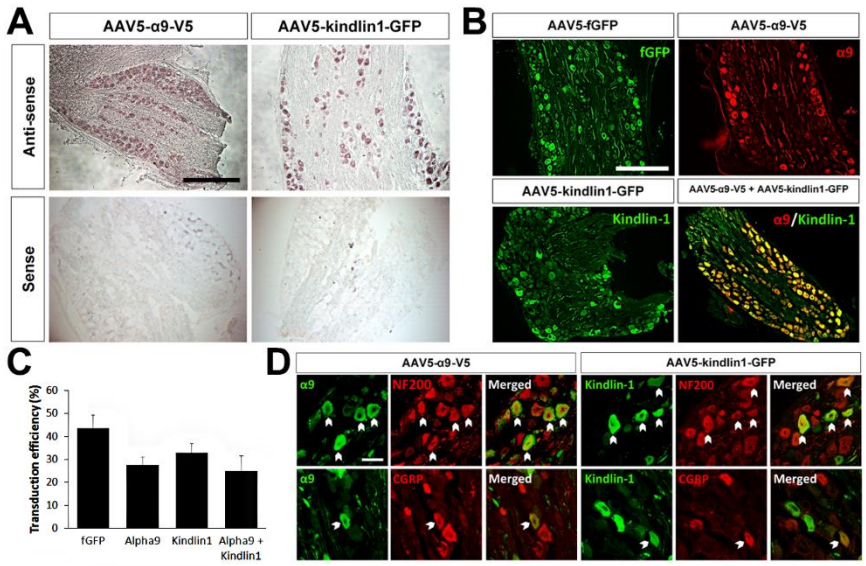

Figure 3. Expression of α9 integrin and kindlin-1 in DRG neurons 4 weeks after direct injection

(A) *In situ* hybridization of AAV5-α9-V5 or AAV5-kindlin1-GFP injected DRG sections, labeled with anti-sense and sense probes for α9 integrin or kindlin-1. Scale bar is 500 µm. **(B)** DRG sections injected with AAV5-fGFP, AAV5-α9-V5 and/or AAV5-kindlin1-GFP. Scale bar is 500 µm. **(C)** Transduction efficiencies of AAV5-fGFP, AAV5-α9-V5 and AAV5-kindlin1-GFP in DRG neurons, expressed as mean ± SEM, n=5. **(D)** DRG sections injected with AAV5-α9-V5 or AAV5-kindlin1-GFP, co-labeled with antibodies to NF200 or CGRP. Scale bar is 50 µm.

Figure 4

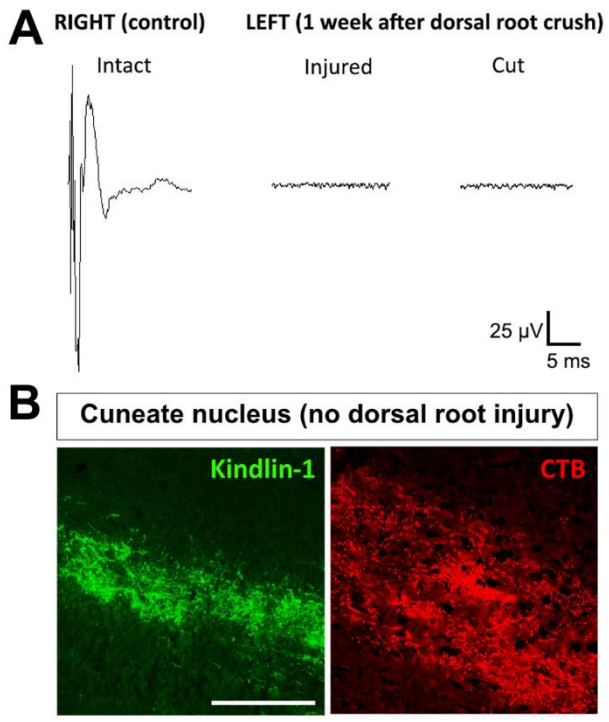

Figure 4. Dorsal root crush injury denervates the spinal cord

(A) Electrophysiological recordings at the right C7 dorsal horn with right C7 dorsal root intact as an internal control, and the left C7 dorsal horn with left C7 dorsal root 1 week after injury and then cut subsequently, n=5. **(B)** Section of cuneate nucleus from animals injected with AAV5-kindlin1-GFP or CTB with no dorsal root crush injury. Animals that showed visible CTB and/or kindlin-1 staining in the cuneate nucleus were excluded from all analyses (3 out of 58 animals). Scale bar is 250 µm.

Figure 5

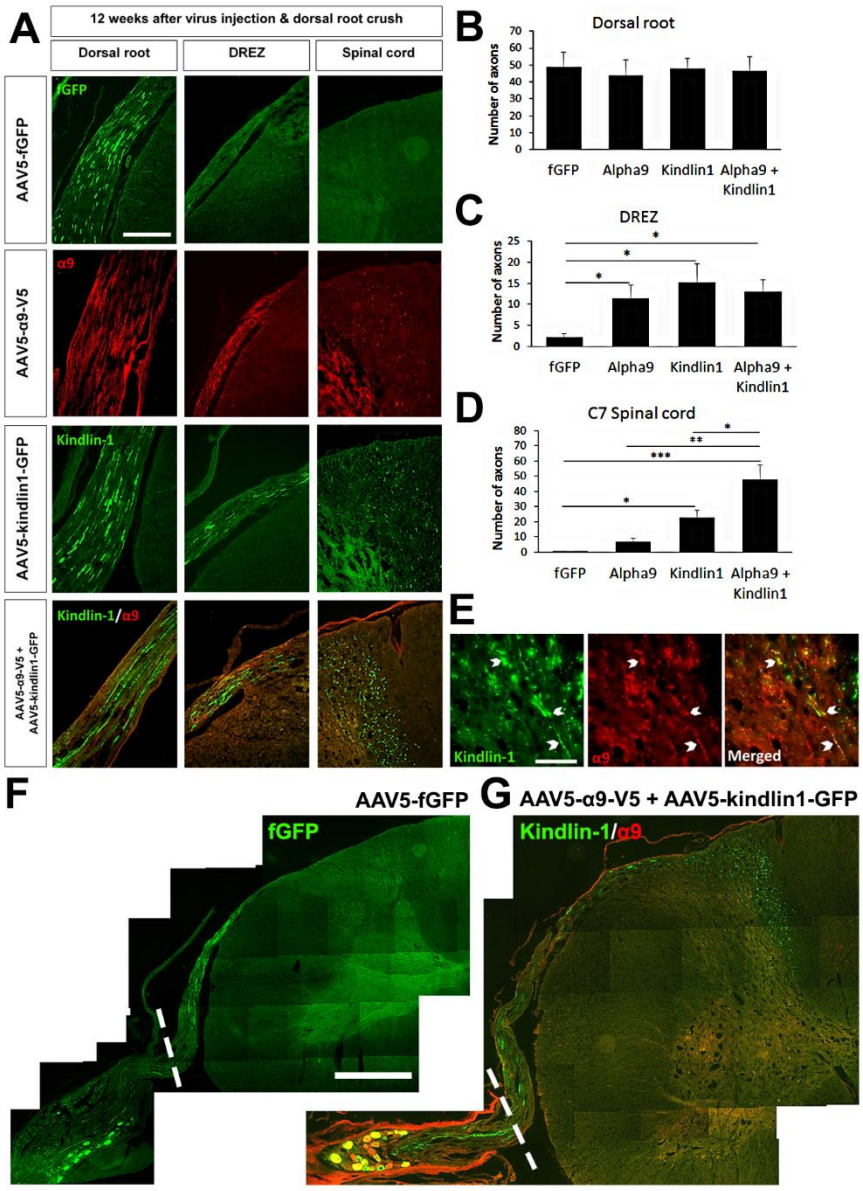
A
12 weeks after virus injection & dorsal root crush
Dorsal root
DREZ
Spinal cord
AAV5-fGFP
fGFP
AAV5-α9-V5
α9
AAV5-kindlin1-GFP
Kindlin-1
AAV5-α9-V5 + AAV5-kindlin1-GFP
Kindlin-1/α9
B
Dorsal root
Number of axons
fGFP
Alpha9
Kindlin1
Alpha9 + Kindlin1
C
DREZ
D
C7 Spinal cord
E
Kindlin-1
α9
Merged
F
AAV5-fGFP
fGFP
G
AAV5-α9-V5 + AAV5-kindlin1-GFP
Kindlin-1/α9

Figure 5. Co-expression of α9 integrin and kindlin-1 promotes sensory axon regeneration into the spinal cord at level C7

(A) Dorsal root, DREZ and spinal cord C7 sections 12 weeks after being injected with AAV5-fGFP, AAV5-α9-V5 and/or AAV5-kindlin1-GFP and followed by dorsal root crush injury. Scale bar is 250 μm. **(B-D)** The number of axons per section in the dorsal root (**B**), DREZ (**C**) and C7 spinal cord (**D**) after 12 weeks of treatment, 3 sections per animal, analyzed by one-way ANOVA and expressed as mean ± SEM, *$p<0.05$, **$p<0.01$ and ***$p<0.001$ were statistically significant, n=10 per group. **(E)** Axons co-expressing kindlin-1 and α9 integrin in the spinal cord. Scale bar is 50 μm. **(F-G)** Spinal cord sections at level C7 of AAV5-fGFP (**F**) or AAV5-α9-V5 + AAV5-kindlin1-GFP (**G**) injected animal 12 weeks after dorsal root crush injury. The white-dotted lines represent the region of dorsal root crush. Scale bar is 650 μm.

Figure 6

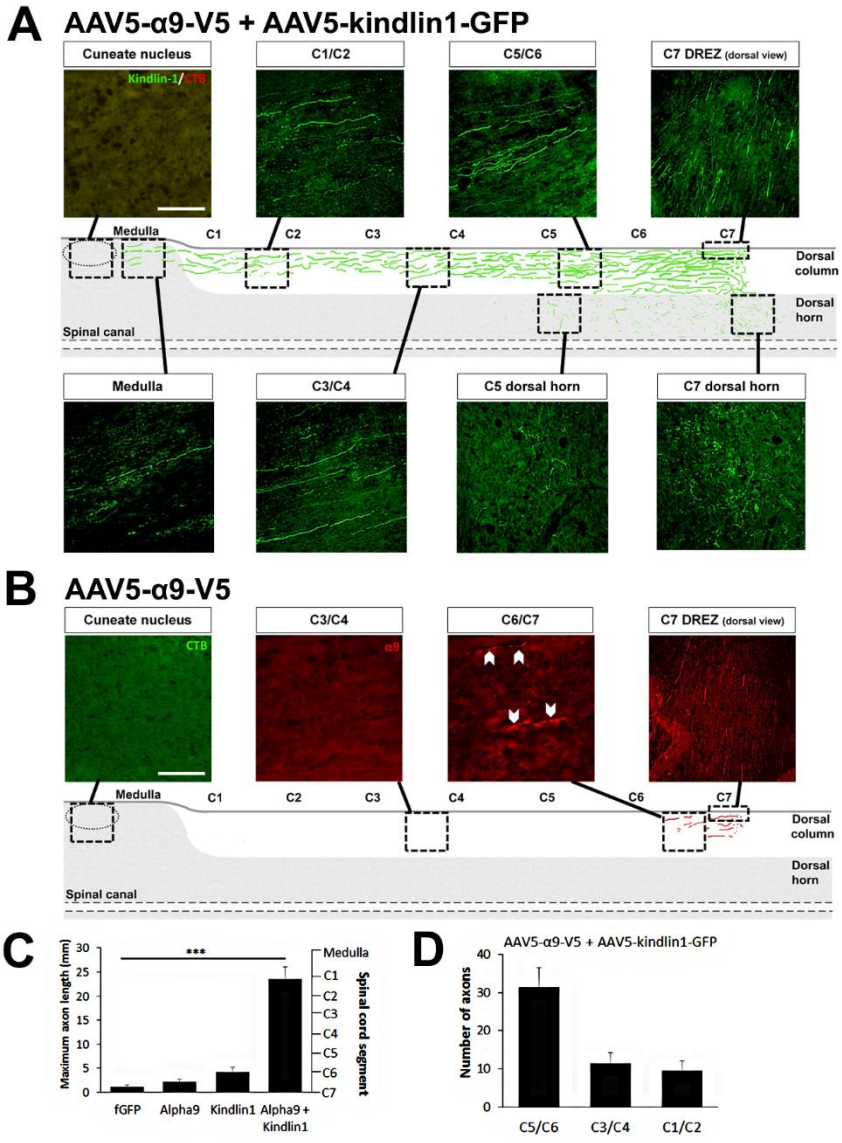
A
AAV5-α9-V5 + AAV5-kindlin1-GFP
Cuneate nucleus
Kindlin-1/CTB
C1/C2
C5/C6
C7 DREZ (dorsal view)
Medulla
C1
C2
C3
C4
C5
C6
C7
Dorsal column
Dorsal horn
Spinal canal
Medulla
C3/C4
C5 dorsal horn
C7 dorsal horn
B
AAV5-α9-V5
Cuneate nucleus
CTB
C3/C4
α9
C6/C7
C7 DREZ (dorsal view)
Medulla
C1
C2
C3
C4
C5
C6
C7
Dorsal column
Dorsal horn
Spinal canal
C
Maximum axon length (mm)
***
Medulla
C1
C2
C3
C4
C5
C6
C7
Spinal cord segment
fGFP
Alpha9
Kindlin1
Alpha9 + Kindlin1
D
AAV5-α9-V5 + AAV5-kindlin1-GFP
Number of axons
C5/C6
C3/C4
C1/C2

Figure 6. Co-expression of α9 integrin and kindlin-1 promotes sensory axon regeneration in the dorsal column up to C1 level and the medulla

(A-B) Diagrams representing a single 14 μm parasagittal spinal cord section of AAV5-α9-V5 + AAV5-kindlin1-GFP (**A**) or AAV5-α9-V5 (**B**) injected animals 12 weeks after dorsal root crush injury, showing regenerating axons in various regions along the spinal cord. Scale bar is 250 μm. The diagrams were produced by drawing the axons from single sections taken from the middle of the dorsal horn into the arrowed squares then interpolating between them. Each dorsal column is approximately 600 μm across or approximately 40 parasagittal 14 μm sections. **(C)** The maximum length (mm) of regenerating axons observed along the spinal cord for each group, analyzed by one-way ANOVA and expressed as mean ± SEM, ***$p<0.001$ was statistically significant, n=5. **(D)** The number of axons per section at C5/C6, C3/C4 and C2/C1 spinal cord segments of the alpha9 + kindlin1 group, expressed as mean ± SEM, n=5.

Figure 7

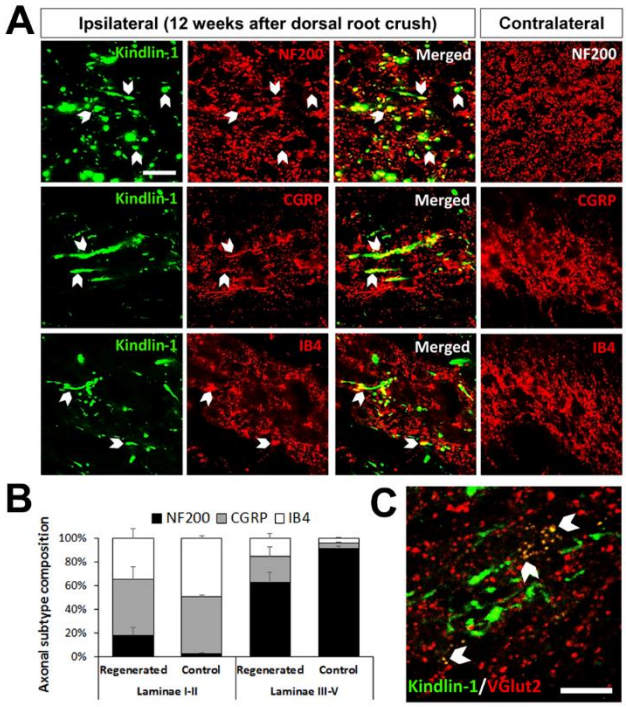

Figure 7. Co-expression of α9 integrin and kindlin-1 promotes axonal re-connections in the spinal cord

(A) Ipsilateral spinal cord C7 sections showing kindlin-1-positive regenerating axons which are immunopositive for NF200 in the dorsal column, CGRP and IB4 in the dorsal horn. The contralateral control side is the corresponding uninjured region of the spinal cord. Scale bar is 50 µm. **(B)** The composition of axonal subtypes NF200, CGRP and IB4 in laminae I-II and laminae III-V of the dorsal horn on the ipsilateral regenerated and contralateral control sides. Results expressed as mean ± SEM, 3 sections per animal, n=5. **(C)** Spinal cord section showing potential synaptic reconnections of kindlin-1-positive axonal terminals with VGlut2-positive neurons in the dorsal horn. Scale bar is 50 µm.

Figure 8

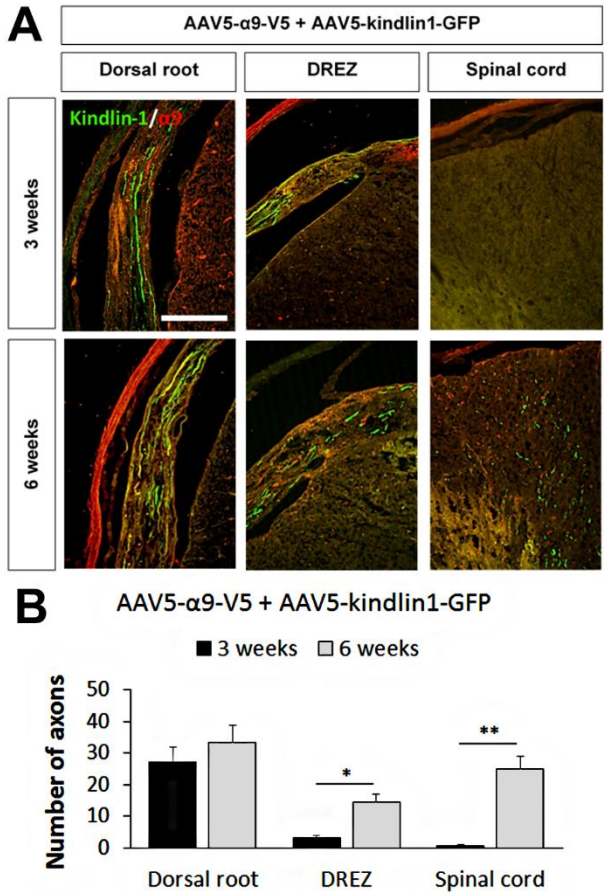

Figure 8. Co-expression of α9 integrin and kindlin-1 promotes sensory axon regeneration in a time-dependent manner

(A) Dorsal root, DREZ and spinal cord C7 sections 3 and 6 weeks after being injected with AAV5-α9-V5 + AAV5-kindlin1-GFP and followed by dorsal root crush injury. Scale bar is 250 µm. **(B)** The number of axons per section in the dorsal root, DREZ and spinal cord after 3 and 6 weeks of treatment, 3 sections per animal, analyzed by Student's t-test and expressed as mean ± SEM, *$p<0.05$ and **$p<0.01$ were statistically significant, n=5.

Figure 9

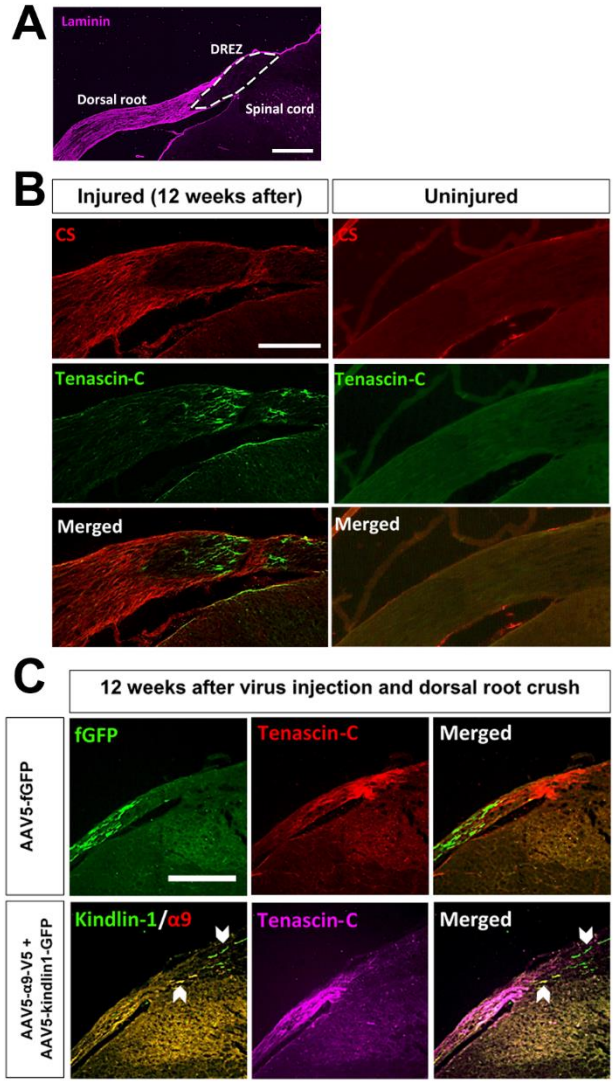
A
Laminin
DREZ
Dorsal root
Spinal cord
B
Injured (12 weeks after)
Uninjured
CS
CS
Tenascin-C
Tenascin-C
Merged
Merged
C
12 weeks after virus injection and dorsal root crush
AAV5-fGFP
fGFP
Tenascin-C
Merged
AAV5-α9-V5 + AAV5-kindlin1-GFP
Kindlin-1/α9
Tenascin-C
Merged

Figure 9. DREZ is a barrier for DRG axon regeneration

(A) The DREZ (*white-bordered area*) is defined as the segment in the dorsal root which is immunonegative for laminin. Scale bar is 500 µm. **(B)** Spinal cord section labeled with antibodies to chondroitin sulfate (CS) chain and tenascin-C to show the upregulation of CSPGs in the injured dorsal root and tenascin-C in the DREZ 12 weeks after dorsal root crush injury. Scale bar is 250 µm. **(C)** Spinal cord section of AAV5-fGFP or AAV5-α9-V5 + AAV5-kindlin1-GFP injected animals 12 weeks after dorsal root crush injury, showing fGFP-expressing axons do not grow into the tenascin-C-rich DREZ, whereas α9 integrin and kindlin-1-expressing axons grow beyond the tenascin-C-rich DREZ and into the spinal cord. Scale bar is 250 µm.

Figure 10

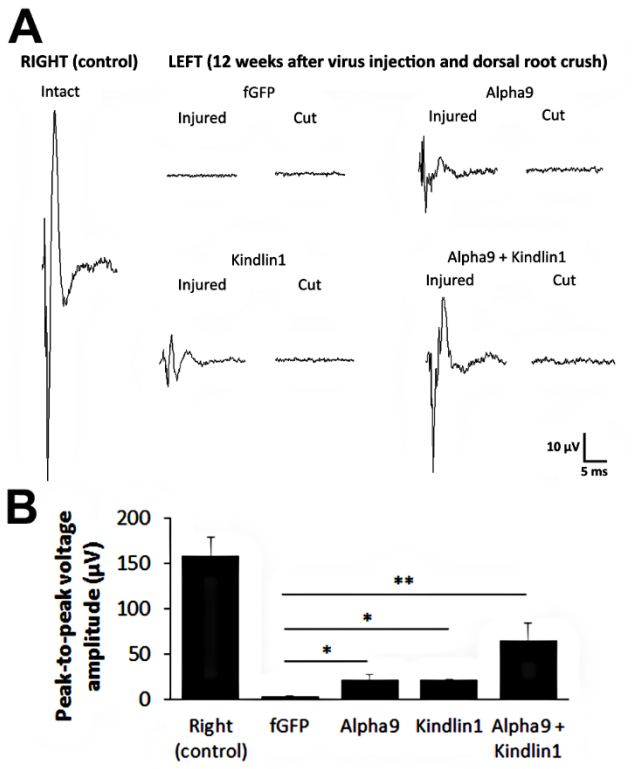

Figure 10. Treatment with α9 integrin and kindlin-1 promotes electrophysiological improvement

(A) Electrophysiological recordings at the right C7 dorsal horn with right C7 dorsal root intact as an internal control, and the left C7 dorsal horn with left C7 dorsal root injured (12 weeks after crush/regeneration) and then cut in fGFP, alpha9, kindlin1, and alpha9 + kindlin1 treatment groups. **(B)** Peak-to-peak voltage amplitude of the intact/injured recordings from each treatment group, analyzed by one-way ANOVA and expressed as mean ± SEM, *$p<0.05$ and **$p<0.01$ were statistically significant, n=5.

Figure 11

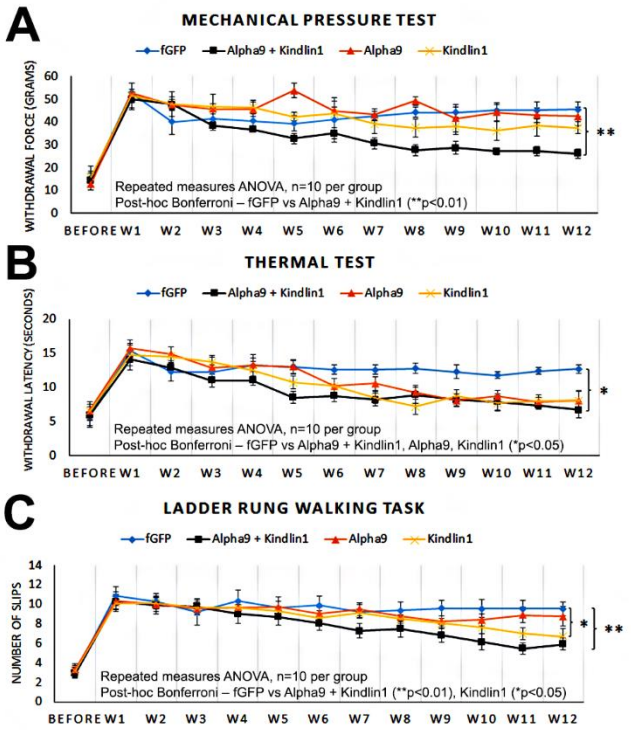

Figure 11. Treatment with α9 integrin and kindlin-1 promotes sensory behavioral recovery

(A-C) Mechanical pressure test (**A**), thermal test (**B**) and ladder rung walking task (**C**) on the experimental left forepaw, before the surgery and during weeks 1-12 after surgery. The results were analyzed by repeated measures ANOVA and expressed as mean ± SEM, *p<0.05 and **p<0.01 were statistically significant, n=10 per group.